

MATERIALS OF THE CONFERENCE  
“NANOMATERIALS AND LIVING SYSTEMS” (NLS-2018), KAZAN, 2018

## Hybrid Nanosystems Based on an Antibacterial Preparation of Dioxydine and Metal Nanoparticles (Ag and Cu) Included in Biopolymer Cryostructures

T. I. Shabatina<sup>a\*</sup>, O. I. Vernaya<sup>a</sup>, A. V. Nuzhdina<sup>a</sup>, N. D. Zvukova<sup>b</sup>, V. P. Shabatin<sup>a</sup>, A. M. Semenov<sup>a</sup>, V. I. Lozinskii<sup>b</sup>, and M. Ya. Mel'nikov<sup>a</sup>

<sup>a</sup> *Moscow State University, Moscow, 119991 Russia*

<sup>b</sup> *Nesmeyanov Institute of Organoelement Compounds, Russian Academy of Sciences, Moscow, 119991 Russia*

\**e-mail: tatyashabatina@yandex.ru*

Received February 20, 2018; in final form, April 27, 2018

**Abstract**—Cryochemical approaches have been used to synthesize hybrid systems consisting of a cryomodified  $\beta$  form of dioxydine (particle size of 30–350 nm) and silver or copper nanoparticles (average size of 5–18 nm). These hybrid composites and their precursors are incorporated into biopolymer cryostructures based on gelatin and calcium alginate. Hybrid composites based on metals and antibacterial drugs are very active in the inhibition of growth of *E. coli* 52, *S. aureus* 144, and *M. cyaneum* 98 in comparison with their separate components.

DOI: 10.1134/S1995078018020106

### INTRODUCTION

The success of modern pharmacological therapy is associated not only with optimizing existing pharmacological therapy, but also with the development of fundamentally new drug forms. The efficiency of action of pharmacopoeial drugs may be improved, in particular, by developing new hybrid drugs containing known preparations and nanoscale biologically active inorganic nanoparticles [1–3]. Preparations with the controlled release of drug substances, including drug forms with prolonged action whose release takes longer in comparison with the usual drug form when administered to the body, are promising [4–7]. The development of drug forms with prolonged action also results in a decrease in the peak concentration and elimination of temporary fluctuations in the concentration of the active substance in the blood and tissues, which are unavoidable with the periodically repeated use of medical preparations. Such drug forms can be prepared by binding a pharmacologically active component to a biopolymer matrix, which provides for a gradual release of the drug from it and prolonged maintenance of the desired concentration of the active drug in the body or locally in a particular target organ. The systems based on gelatin and calcium alginate may be used as possible biopolymer matrices, depots for drugs [8–11].

The goal of this work was to synthesize hybrid nanocomposites based on the antibacterial preparation of dioxydine and metal nanoparticles (silver and

copper), incorporate the nanocomposites into alginate and gelatinous cryostructures capable of prolonged release, and determine the antibacterial activity of these hybrid drug nanoforms against bacterial cells of *E. coli* 52, *S. aureus* 144, and *M. cyaneum* 98.

### EXPERIMENTAL

The substance of dioxydine corresponding to the pharmacopoeial article 42-2308-97, colloid silver of the KND-S-K brand (TU 9154-024-74107096-2008), basic copper carbonate, formic acid, copper chloride II, and hydrazine hydrate (analytically pure) were used without additional purification. Copper nanoparticles were obtained by the reduction of highly dispersed anhydrous copper formate with hydrogen at 180°C for 90 min [12] and the reduction of the aqueous solution of copper chloride with hydrazine hydrate [13]. The low-temperature synthesis of gelatinous and Ca-alginate cryostructures was carried out as described in [14, 15].

A highly dispersed powder of dioxydine and hybrid nanocomposites of dioxydine with silver (Ag/dioxydine) or copper (Cu/dioxydine) nanoparticles was prepared by the dispersion of an aqueous solution containing dioxydine and metal nanoparticles (1 wt % dioxydine and 0.005 wt % Ag or 0.02 wt % Cu) through a pneumatic atomizer into liquid nitrogen; the frozen solutions were subsequently subjected to cryosublimation drying for 24 h [16–19]. Dioxydine, as

well as Ag/dioxydine and Cu/dioxydine nanocomposites, were included in the disks of cryostructures as follows. Sponge discs were immersed in aqueous solutions of dioxydine and metal nanoparticles (1 wt % dioxydine and 0.02 wt % Ag or 0.02 wt % Cu). The discs were subsequently removed from the solution, frozen with liquid nitrogen, and subjected to cryosublimation drying for 24 h. The samples based on calcium alginate (Ag/dioxydine/alginate and Cu/dioxydine/alginate) contained 14 wt % dioxydine and 0.56 wt % of the metal. The samples based on gelatin (Ag/dioxydine/gelatin and Cu/dioxydine/gelatin) contained 11.5 wt % dioxydine and 0.46 wt % of the metal. Copper nanoparticles obtained by the reduction of the anhydrous copper formate (particle size of 5–50 nm) with hydrogen were used for hybrid Cu/dioxydine and Cu/dioxydine/alginate composites. Copper nanoparticles obtained by the reduction of copper chloride with hydrazine hydrate (particle size of 1–9 nm) were used for Cu/dioxydine/gelatin.

X-ray phase analysis (XPA) of the samples was carried out with a Rigaku D/MAX-2500 diffractometer (Rigaku, Japan) at  $\text{CuK}\alpha$  radiation ( $\lambda = 1.54056 \text{ \AA}$ ). IR spectra of the samples were obtained with a Bruker Tensor II spectrometer (Germany) equipped with the ATR platinum device in the interval from 4000 to  $400 \text{ cm}^{-1}$ . The IR spectra of powdered samples was registered by the diffuse reflection technique. UV spectra of aqueous solutions of the samples (0.01 wt %) were measured with a Jasco V-770 spectrophotometer (Jasco, Japan) in the range from 200 to 700 nm. The kinetics of the release of dioxydine from cryostructures was monitored spectrophotometrically with a Jasco V-770 spectrophotometer (Jasco, Japan) at  $\lambda = 360 \text{ nm}$ .

The microstructure of the samples was studied by transmission electron microscopy (TEM) using a LEO 912 AB Omega electron microscope (ZEISS, Germany) at magnification  $\times 80$ – $\times 500000$  and scanning electron microscopy (SEM) with a Phenom scanning electron microscope (FEI Company, Germany) at magnification  $\times 20$ – $\times 4000$ . The specific surface area ( $S_{\text{sp}}$ ) of the samples was determined by the low-temperature adsorption–thermal desorption of argon on a laboratory unit based on a Khrom 5 chromatograph. Preliminarily adsorbed gases were removed from the surface of the samples with a vacuum unit. The average particle size ( $a$ ) of dioxydine was calculated with the formula  $a = 6/(\rho S_{\text{sp}})$ , where  $\rho$  is the density of dioxydine.

The antibacterial activity of various forms of dioxydine, as well as Ag/dioxydine and Cu/dioxydine hybrid nanocomposites, in comparison with the original dioxydine and solutions of colloid silver and copper, was determined by the disk diffusion method [20]. Compressed tablets (0.1 g, 0.5 mm, and 0.5 atm), discs of filter paper (Krasnaya Lenta brand) (diameter of

5 mm), and disks of alginate and gelatinous cryostructures (diameter of 4 mm and height of 2 mm) were used. Bacterial cells obtained from the collection of bacterial cultures of the Department of Microbiology of the Faculty of Biology at Moscow State University were used as test cultures. These were *E. coli* 52, *S. aureus* 144, and *M. cyaneum* 98. The experiments were carried out in Petri dishes containing 20 mL of agar nutrient medium dried for 24 h (the thickness of the layer of the medium was 4 mm). Measurements of the growth-inhibition zones (GIZ) of the test cultures were performed after 16 h of incubation. Statistically significant results were obtained with ninefold replicates of the GIZ measurements for each series of samples.

## RESULTS AND DISCUSSION

The samples were characterized by physical and chemical analysis to reveal their chemical composition. NMR- $^1\text{H}$  spectra of the original dioxydine ( $\text{D}_2\text{O}$ )  $\delta$ : 4.93–5.21 (m, 4H,  $2^*\text{CH}_2$ ), 7.85–8.05 (m, 2H, H Ar), and 8.38–8.52 (m, 2H, H Ar), as well as of the cryomodified preparation ( $\text{D}_2\text{O}$ )  $\delta$ : 4.95–5.25 (m, 4H,  $2^*\text{CH}_2$ ), 7.86–8.05 (m, 2H, H Ar), and 8.35–8.50 (m, 2H, H Ar), confirm that the substance obtained during cryomodification retains its chemical composition. The UV spectra of aqueous solutions of Ag/dioxydine and Cu/dioxydine composites include an intense absorption band at 250 nm (241 and 259 nm doublet) related to the  $\pi \rightarrow \pi^*$  electron transfer of carbon atoms of the aromatic system and a low-intensity band at 375 nm related to the  $n \rightarrow \pi^*$  transfer of n-electrons of the nitrogen atom [19]. IR spectra of the original and cryomodified dioxydine showed some differences. Thus, the vibration band of the quinoxaline ring for the original pharmacopeic dioxydine was at  $1506 \text{ cm}^{-1}$ , the vibration bands of the C–H aromatic ring had a peak at  $971 \text{ cm}^{-1}$ , two doublets were at 1117 and  $1113 \text{ cm}^{-1}$  and 1152 and  $1160 \text{ cm}^{-1}$ , and the C–O–H vibration band was also doublet at 1280 and  $1288 \text{ cm}^{-1}$ . At the same time, in the case of cryomodified dioxydine, the vibration band of the quinoxaline ring was at  $1510 \text{ cm}^{-1}$ ; the C–H vibration bands of the benzene ring were observed at 975, 113, and  $1160 \text{ cm}^{-1}$ , while the C–O–H vibration band was at  $1288 \text{ cm}^{-1}$ . X-ray diffraction patterns, as well as interplanar distances ( $d$ ,  $\text{\AA}$ ) and intensities ( $I_{\text{rel}}$ , %), calculated on the basis of the original dioxydine ( $d$ ,  $\text{\AA}$ ,  $I_{\text{rel}}$ , %): 8.638, 100.0%; 7.897, 21.8%; 7.508, 68.4%; 6.846, 12.2%; 3.299, 24.8%; and 2.242, 16.8%) and cryomodified dioxydine ( $d$ ,  $\text{\AA}$ ,  $I_{\text{rel}}$ , %): 8.740, 100.0%; 8.026, 94.2%; 6.899, 57.8%; 6.288, 50.9%; 5.978, 43.4%; 3.358, 99.3%; and 3.304, 67.6%), proved to be different. This indicates that another crystalline form of dioxydine, its  $\beta$  form, was obtained during cryomodification.

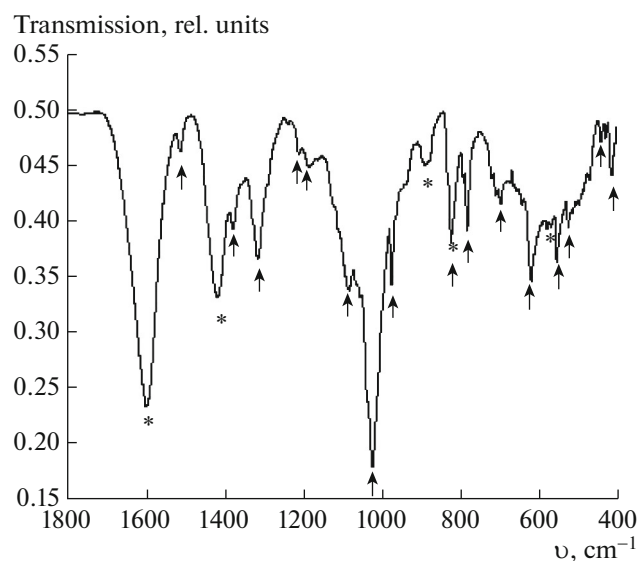


**Fig. 1.** IR spectra of alginate cryostructure after the inclusion of dioxydine (\* absorption bands of the alginate matrix; ↑ absorption bands of dioxydine).

The specific surface was determined by the low-temperature adsorption of argon and the average particle size of the original ( $0.7 \text{ m}^2/\text{g}$ ,  $5700 \text{ nm}$ ) and cryomodified dioxydine ( $25.8 \text{ m}^2/\text{g}$ ,  $155 \text{ nm}$ ) was calculated. The decrease in the particle size of dioxydine during cryomodification was confirmed by TEM data, on the basis of which it can be concluded that the particle size of the obtained form of dioxydine was within  $30\text{--}300 \text{ nm}$  (the average size of  $170 \text{ nm}$ ). The data on low-temperature adsorption of argon are probably more reliable, since the photomicrographs obtained by the TEM method show that the particles of dioxydine partially melted under the action of the electron beam (despite the fact that a low-energy version of the method was used).

The UV spectra of aqueous solutions of Ag/dioxydine and Cu/dioxydine composites included maxima at  $\lambda_{\text{max}} = 250$  and  $375 \text{ nm}$ , which belonged to dioxydine. In the case of Ag/dioxydine composites at  $405 \text{ nm}$ , absorption caused by the surface plasmon resonance of silver nanoparticles was observed and its low intensity was associated with the low silver content in the sample. The absence of a band corresponding to the plasmon absorption of copper nanoparticles in the UV spectrum of the aqueous solution of Cu/dioxydine composites is associated with the low intensity of this absorption in comparison with dioxydine and the small content of copper nanoparticles in the sample. The bands belonging to dioxydine were also present in the UV spectra of aqueous extracts of the Ag/dioxydine/alginate, Ag/dioxydine/gelatin, Cu/dioxydine/alginate, and Cu/dioxydine/gelatin samples.

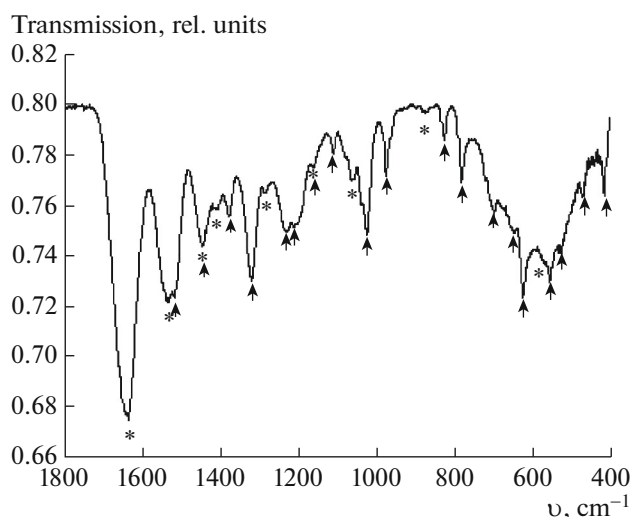


**Fig. 2.** IR spectra of gelatinous cryostructure after the inclusion of dioxydine (\* absorption bands of the gelatinous matrix; ↑ absorption band of the activated dioxydine).

The IR spectra of Ag/dioxydine and Cu/dioxydine composite powders were identical to the IR spectrum of the cryomodified dioxydine. The IR spectra of the Ag/dioxydine/gelatin and Ag/dioxydine/alginate systems, as well as of Cu/dioxydine/gelatin and Cu/dioxydine/alginate ones, were a superposition of IR spectra of the cryomodified dioxydine and the matrix used. Wide bands of gelatin and alginate at  $534$  and  $550 \text{ cm}^{-1}$ , respectively, overlap with narrower bands of dioxydine (Figs. 1, 2).

Figure 3 shows the kinetic curves for the release of dioxydine from biopolymer matrices. The release of dioxydine from the alginate and gelatinous matrices occurred within 40 and 60 min, respectively.

According to the data of transmission electron microscopy (TEM), Ag/dioxydine and Cu/dioxydine nanocomposites consisted of organic particles ( $50\text{--}350 \text{ nm}$  in size), which included nanoscale silver (with an average size of  $10 \text{ nm}$ ) or Cu ( $18 \text{ nm}$  in size) particles. The specific surface area and calculated average particle size for Ag/dioxydine composites were  $31 \text{ m}^2/\text{g}$  and  $130 \text{ nm}$ , respectively. They were  $24 \text{ m}^2/\text{g}$  and  $166 \text{ nm}$  for Cu/dioxydine composites. Thus, the values of the average particle size obtained by the low-temperature adsorption of argon agreed with the data obtained by TEM.

SEM photomicrographs (Figs. 4a, 5a) indicated that alginate and gelatinous cryostructures are wide-porous matrices with a pore size of tens of micrometers. The inclusion of dioxydine and metal nanoparticles did not significantly affect their size, which, along with IR spectra, supported the fact that dioxydine, included in the biopolymer cryostructures, was chemically identical to its cryomodified  $\beta$  form. This

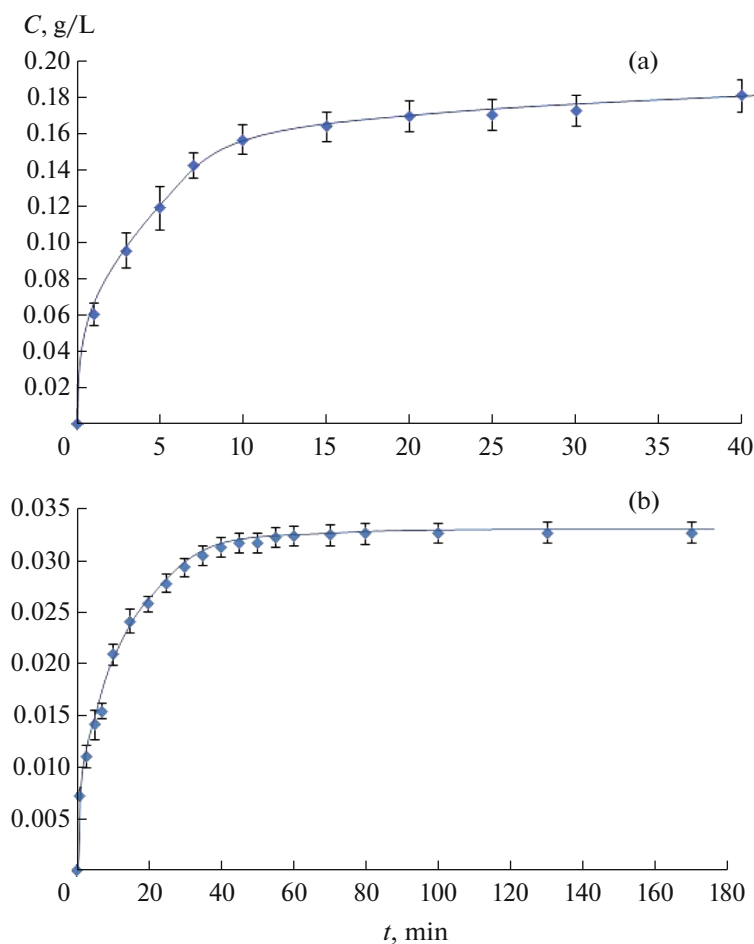


Fig. 3. (Color online) Kinetic curves for the release of dioxydine from alginate (a) and gelatinous (b) matrices.

also explains the relatively high rate of drug release from the biopolymer matrix (40–60 min). In the future, the change in the structure of the matrix caused by variations in the conditions for its synthesis can be used by us to reduce the rate of dioxydine release from the obtained nanoforms, as well as to obtain a prolonged effect of the controlled release of the drug component.

TEM photomicrographs (Figs. 4b, 4c, 5b, 5c) of the Ag/dioxydine/alginate, Cu/dioxydine/alginate, Ag/dioxydine/gelatin, and Cu/dioxydine/gelatin nanocomposites show the following. Organic matrices

contain silver nanoparticles with a size varying from 2 to 30 nm or copper nanoparticles with a size ranging from 1 to 9 nm (in the case of the Cu/dioxydine/gelatin system) and from 5 to 50 nm (in the case of the Cu/dioxydine/alginate system).

The antibacterial activity of the various forms of dioxydine and hybrid nanosystems based on it was determined for microbial cells of *E. coli* 52, *S. aureus* 144, and *M. cyaneum* 98. The data are summarized in Tables 1–3. A cryochemical modification of dioxydine with a change in its size and structure results in an increase in its antibacterial activity (Table 1). The antibacterial activity of hybrid composites of metal and dioxydine nanoparticles was also higher than that of individual metal nanoparticles and dioxydine, both in the case of tests by the standard disc-diffusion method and in the case of using biopolymer cryostructures for tests with disks (Tables 2, 3). Thus, the hybrid systems of dioxydine and metal nanoparticles show a synergistic increase in antibacterial activity against the bacterial strains used, in comparison with the action of the individual drug components.

**Table 1.** Growth-inhibition zone (GIR) of *E. coli* 52, *S. aureus* 144, and *M. cyaneum* 98 around compressed tablets of various dioxydine forms

Bacterial strain	GIR, original dioxydine, mm	GIR, cryomodified dioxydine, mm
<i>E. coli</i> 52	$34.0 \pm 1.0$	$38.3 \pm 1.5$
<i>S. aureus</i> 144	$33.0 \pm 1.0$	$37.3 \pm 0.6$
<i>M. cyaneum</i> 98	$26.3 \pm 0.6$	$36.3 \pm 1.0$

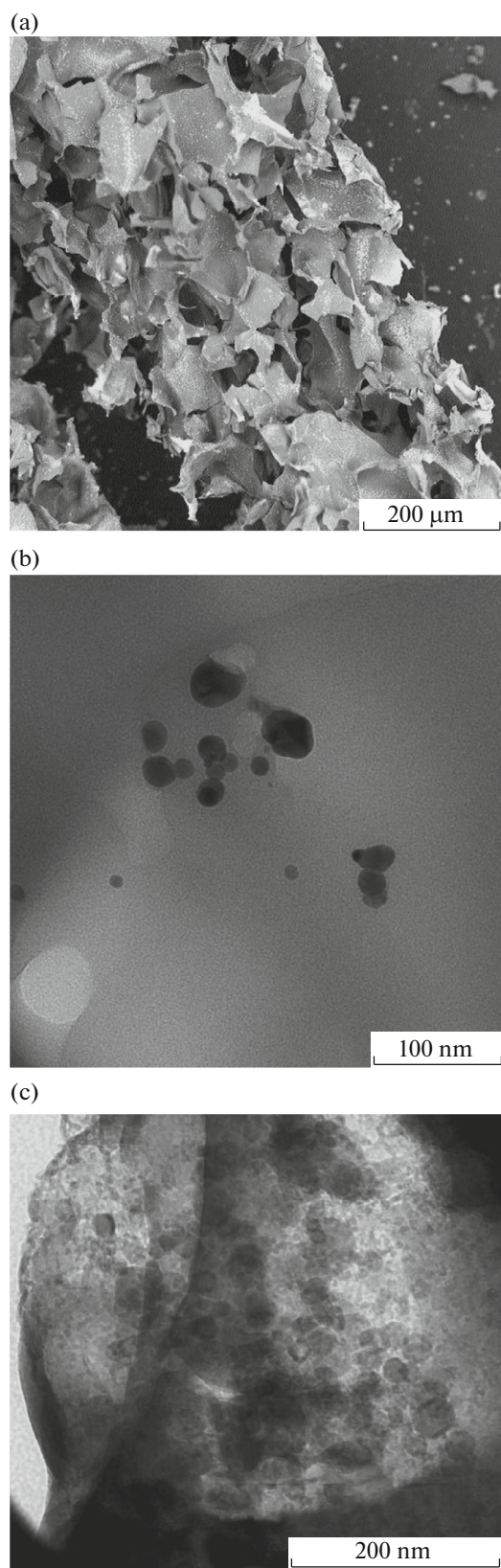


**Fig. 4.** Scanning electron microscopy of alginate cryostructure (a) and transmission electron microscopy of hybrid Ag/dioxydine/alginate (b) and Cu/dioxydine/alginate (c) nanosystems.

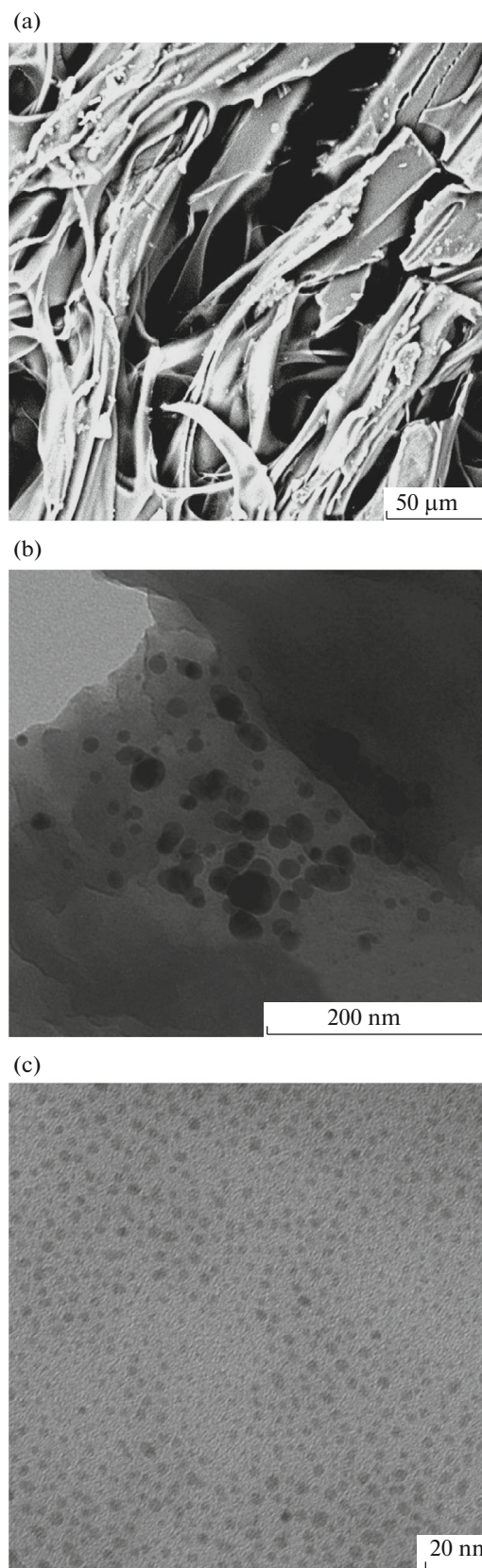


**Fig. 5.** Scanning electron microscopy of gelatinous cryostructure (a) and transmission electron microscopy of hybrid Ag/dioxydine/gelatin (b) and Cu/dioxydine/gelatin (c) nanosystems.

**Table 2.** GIR of *E. coli* 52, *S. aureus* 144, and *M. cyaneum* 98 around discs of filter paper impregnated with the solutions\* of samples

Bacterial strain	GIR, Ag, mm	GIR, Cu, mm	GIR, dioxydine, mm	GIR, Ag/dioxydine, mm	GIR, Cu/dioxydine, mm
<i>E. coli</i> 52	0	0	26 ± 1.2	36.7 ± 0.6	32.1 ± 1.2
<i>S. aureus</i> 144	0	0	30.3 ± 0.6	37.4 ± 0.6	33.0 ± 1.2
<i>M. cyaneum</i> 98	0	0	26.1 ± 0.8	36.3 ± 0.6	31.5 ± 0.8

\*Dioxydine, 0.3 wt %; Ag, 0.0015 wt %; Cu, 0.006 wt %.

**Table 3.** GIR of *E. coli* 52 around dioxydine, Cu and Ag nanoparticles, and hybrid nanocomposites of dioxydine and metal (Ag and Cu) nanoparticles incorporated into biopolymer cryostructures

Cryostructural matrix	GIR, Cu, mm	GIR, Ag, mm	GIR, dioxydine, mm	GIR, Cu/dioxydine, mm	GIR, Ag/dioxydine, mm
Alginate	0	10.0 ± 0.6	20.0 ± 0.6	22.1 ± 1.2	23.0 ± 1.8
Gelatin	0	4.0 ± 1.2	35.0 ± 0.6	37.3 ± 1.2	38.1 ± 1.2

## CONCLUSIONS

New hybrid nanoforms were obtained by cryochemical synthesis. They were based on a cryo-modified antibacterial preparation of dioxydine with a crystalline structure different from the original pharmacopeic dioxydine and contained nanoscaled particles (with an average size of 5–18 nm) of biologically active metals (silver and copper) included in the cryo-structured biopolymer matrices of gelatin and calcium alginate. Hybrid nanosystems synthesized in this study showed high activity against *E. coli* 52, *S. aureus* 144, and *M. cyaneum* 98 in comparison with individual components. The incorporation of the obtained hybrid nanosystems into biopolymer cryostructures does not result in the disappearance of the observed antibacterial effect caused by specific intermolecular or covalent interactions between the components of the drug composition and the chemical matter of the matrix, for instance. Moreover, it also provides for a gradual release of the active drug components from the wide-pore polymer matrix, i.e., the prolonged action of the synthesized hybrid nanosystems. The antibacterial hybrid nanocomposites and transport systems containing them may be used in the development of new direct-delivery drug preparations and the controlled release of drug components.

## ACKNOWLEDGMENTS

This work was supported by the Russian Science Foundation, project no. 16-13-10365.

## REFERENCES

1. A. Gupta, N. M. Saleh, R. Das, R. F. Landis, A. Bigdeli, K. Motamedchaboki, A. R. Campos, K. Pomeroy, M. Mahmoudi, and V. M. Rotello, "Synergistic antimicrobial therapy using nanoparticles and antibiotics for the treatment of multidrug-resistant bacterial infection," *Nano Futures* **1**, 015004 (2017).
2. P. Li, J. Li, C. Wu, and Q. Wu, "Synergistic antibacterial effects of  $\beta$ -lactam antibiotic combined with silver nanoparticles," *Nanotechnology* **16**, 1912–1917 (2005).
3. X. Dong, M. Al. Awak, N. Tomlinson, Y. Tang, Y.-P. Sun, and L. Yang, "Antibacterial effects of carbon dots in combination with other antimicrobial reagents," *PLoS One* **12**, e0185324 (2017).
4. R. A. Mitran, L. Bajenaru, and M. G. Moisescu, "Controlling drug release from mesoporous silica through an amorphous, nanoconfined 1-tetradecanol layer," *Eur. J. Pharm. Biopharm.* **127**, 318–325 (2018).
5. C. Ding and Z. Li, "A review of drug release mechanisms from nanocarrier systems," *Mater. Sci. Eng., C* **76**, 1440–1453 (2017).
6. A. J. Sami, M. Khalid, T. Jamil, S. Aftab, S. A. Mangat, A. R. Shakoori, and S. Iqbal, "Formulation of novel chitosan guar gum based hydrogels for sustained drug release of paracetamol," *Int. J. Biological Macromol.* **108**, 324–332 (2018).
7. T. Ito, T. Takami, Y. Uchida, and Y. Murakami, "Chitosan gel sheet containing drug carriers with controllable drug-release properties," *Colloid Surf., B* **163**, 257–265 (2018).
8. M. S. Hasnain, A. K. Nayak, M. Singh, M. Tabish, and J. Ara, "Alginate-based bipolymeric-nanobioceramic composite matrices for sustained drug release," *Int. J. Biol. Macromol.* **83**, 71–77 (2016).
9. R. Jalababu, S. Veni, and K. V. N. S. Reddy, "Synthesis and characterization of dual responsive sodium alginate-g-acryloyl phenylalanine-poly n-isopropyl acrylamide smart hydrogels for the controlled release of anticancer drug," *J. Drug Deliv. Sci. Technol.* **44**, 190–204 (2018).
10. R. A. Bini, M. F. Silva, L. C. Varanda, M. A. Silva, and C. A. Dreiss, "Soft nanocomposites of gelatin and poly(3-hydroxybutyrate) nanoparticles for dual drug release," *Colloid Surf., B* **157**, 191–198 (2017).

11. A. Talebian and A. Mansourian, "Release of vancomycin from electrospun gelatin/chitosan nanofibers," *Mater. Today: Proc.* **4**, 7065–7069 (2017).
12. O. I. Vernaya, V. V. Epishev, M. A. Markov, V. A. Nuzhdina, V. V. Fedorov, V. P. Shabatin, and T. I. Shabatina, "Synthesis of copper nanoparticles by thermal decomposition of anhydrous copper formate," *Mosc. Univ. Chem. Bull.* **72**, 267–268 (2017).
13. S. V. Saikova, S. A. Vorob'ev, R. B. Nikolaeva, and Yu. L. Mikhlin, "Conditions for the formation of copper nanoparticles by reduction of copper(II) ions with hydrazine hydrate solutions," *Russ. J. Gen. Chem.* **80**, 1122–1127 (2010).
14. V. I. Lozinsky, V. K. Kulakova, R. V. Ivanov, A. Yu. Petrenko, O. Yu. Rogulska, and Yu. A. Petrenko, "Cryostructuring of polymer systems. 47. Preparation of wide porous gelatin-based cryostructurates in sterilizing organic media and assessment of the suitability of thus formed matrices as spongy scaffolds for 3D cell culturing," *E-Polymers* **18**, 172–176 (2018).
15. I. A. Rodionov, N. V. Grinberg, T. V. Burova, V. Ya. Grinberg, T. I. Shabatina, and V. I. Lozinsky, "Cryostructuring of polymer systems. 44. Freeze-dried and then chemically cross-linked wide porous cryostructurates based on serum albumin," *E-Polymers* **17**, 263–274 (2017).
16. O. I. Vernaya, V. P. Shabatin, A. M. Semenov, and T. I. Shabatina, "Obtaining ultradispersed dioxidine powder modified," *Mosc. Univ. Chem. Bull.* **71**, 291–298 (2016).
17. O. I. Vernaya, V. P. Shabatin, T. I. Shabatina, D. I. Khvatov, A. M. Semenov, T. P. Yudina, and V. S. Danilov, "Cryochemical modification, activity, and toxicity of dioxidine," *Russ. J. Phys. Chem. A* **91**, 229–232 (2017).
18. O. I. Vernaya, D. I. Khvatov, A. V. Nuzhdina, V. V. Fedorov, V. P. Shabatin, A. M. Semenov, and T. I. Shabatina, "Cu/dioxidine hybrid nanocomposites," *Mosc. Univ. Chem. Bull.* **71**, 224–226 (2016).
19. O. I. Vernaya, V. P. Shabatin, A. M. Semenov, and T. I. Shabatina, "Cryochemical synthesis and antibacterial activity of a hybrid composition based on Ag nanoparticles and dioxidine," *Mosc. Univ. Chem. Bull.* **72**, 6–9 (2017).
20. G. G. Onishchenko, "Determination of the sensitivity of microorganisms to antibacterial drugs," *Methodical Instructions* (Moscow, 2004) [in Russian].

*Translated by A. Panyushkina*